Available online at www.sciencedirect.com
SCIENCE DIRECT

Thermochimica Acta 439 (2005) 68–73

thermochimica acta

www.elsevier.com/locate/tca

Comparison of model-free kinetic methods for modeling the cure kinetics of commercial phenol–formaldehyde resins

Jinwu Wang, Marie-Pierre G. Laborie*, Michael P. Wolcott

Wood Materials and Engineering Laboratory, Department of Civil and Environmental Engineering, Washington State University,
P.O. Box 641806, Pullman, WA 99164, USA

Received 8 June 2005; received in revised form 17 August 2005; accepted 1 September 2005
Available online 21 October 2005

Abstract

For many industrial processes it is important to model the cure kinetics of phenol–formaldehyde resoles. Yet the applicability of common model-free kinetic algorithms for the cure of phenolic resins is not known. In this study the ability of the Friedman, Vyazovkin and Kissinger–Akahira–Sunose (KAS) model-free-kinetics algorithms to model and predict the cure kinetics of commercial resoles is compared. The Friedman and Vyazovkin methods generate consistent activation energy dependences on conversion compared to the KAS method. In addition, the activation energy dependency on conversion is of higher amplitude with these two methods than with the KAS method. Hence, the Friedman and Vyazovkin methods are more adequate for revealing the cure steps of commercial PF resoles. Conversely, the KAS algorithm is easily amenable to dynamic cure predictions compared to the Friedman and Vyazovkin methods. Isothermal cure is equally well predicted with the three. As a result, the KAS algorithm is the method of choice for modeling and predicting the cure kinetics of commercial phenolic resoles under various temperature programs.

Keywords: Phenol–formaldehyde; Model-free algorithms; Differential scanning calorimetry (DSC); Cure prediction

1. Introduction

Phenolic resins are widely used as binders in the composites industry, for thermal insulation and molding compounds [1]. As for any thermosets controlling the degree of cure and cure kinetics is critical to designing the manufacturing process and the performance of the end-product. For characterizing cure kinetics differential scanning calorimetry (DSC) is the technique of choice [2]. During a DSC temperature scan phenol–formaldehyde (PF) resoles typically exhibit two exotherms [3–4]. Although a subject of controversy the first exotherm is often ascribed to hydroxymethylphenols (HMPs) formation and condensation while the second exotherm is attributed to dimethylene ether linkages decomposition into methylene linkages between phenolic moieties [3–4]. In addition, commercial PF resoles for wood-based composites are often modified with up to 20 wt.% urea [5] such that their cure may not be adequately modeled with traditional model-fitting kinetic methods [6]. On the other hand, model-free kinetics (MFK) is well suited to portray the kinetics of complex reactions such as the cure of PF resins [6–7]. MFK does not assume any definite form of the reaction and allows for variations in activation energy as the reaction progresses [6]. In fact, both PF and phenol–urea–formaldehyde (PUF) resins have been successfully characterized with MFK using the Kissinger–Akahira–Sunose (KAS) algorithm [8–11]. For PF resoles, changes in activation energy with degree of cure, E_α, helped distinguish two-stages in a highly condensed PF resin. In the first stage E_α increase with degree of cure was ascribed to consecutive and competitive reactions. Following this chemical regime, a decrease in E_α was ascribed to a diffusion-controlled regime [10]. The KAS algorithm could also be used to predict the isothermal cure of PF resins from dynamic tests [10]. Owing to additional cure reactions involving urea, PUF resins exhibited a more complex E_α curve than PF resins [11]. Finally, the effects of water and wood on the cure kinetics of PF resins have also been examined with the KAS method [12–13]. While at low conversion water contributed to reversible cure reactions, it acted as a plasticizer at higher conversion and thus delayed the diffusion control regime enabling more complete cure [12]. Wood was found to accel-

---

* Corresponding author. Tel.: +1 509 335 8722; fax: +1 509 335 5077.
E-mail address: mlaborie@wsu.edu (M.-P.G. Laborie).

0040-6031/$ – see front matter © 2005 Elsevier B.V. All rights reserved.
doi:10.1016/j.tca.2005.09.001

erate the addition reactions in PF resoles while retarding the condensation reactions [13].

To date, all MFK studies on phenolic systems have utilized the KAS algorithm although isoconversional algorithms such as the Vyazovkin [14–15] and Friedman methods [16] are also available. The objective of this research is to evaluate and compare the ability of the Friedman, Vyazovkin and KAS methods for (1) revealing the cure process and (2) predicting the dynamic and isothermal cure behavior of commercial PF resole resins from dynamic test data. In this objective, the cure kinetics of two commercial PF resoles that differ in molecular weight is evaluated with the three MFK methods.

2. Experimental

2.1. Materials

Two PF resoles, tailored as adhesives for oriented strand boards, were obtained from a commercial source. The resins were frozen and stored at −20 °C until use. To determine molecular weights, the resins were acetylated with 1:1 pyridine and acetic anhydride [17] and analyzed by gel permeation chromatography (GPC) in tetrahydrofuran. The GPC system consisted of a Viscotek 270 coupled to a Waters HPLC unit and Jordi Gel polydivinylbenzene mixed bed column with triple detectors. One resin had a weight-average molecular weight (M_w) of 621 g/mol and a polydispersity (M_w/M_n) of 1.41; it was labeled as PF-low. The other resin displayed an $M_w = 6576$ g/mol and $M_w/M_n = 1.72$; it was labeled as PF-high. The resin solid contents were 54.5 and 45.0% for PF-low and PF-high respectively. In addition, elemental analysis [18] showed the presence of 3.7 and 3.9 wt.% nitrogen for PF-high and PF-low, respectively, indicating the presence of urea in both resins.

2.2. Differential scanning calorimetry

A Mettler-Toledo DSC 822^e was used to perform dynamic and isothermal cure experiments. Approximately 13.5 mg of resin was placed in a 30 μl high-pressure gold-plated crucible. Dynamic temperature scans were conducted at five heating rates 2, 5, 10, 20 and 25 °C/min from 25 to 250 °C [10]. Nitrogen was used as a purge gas at a flow rate of 80 ml/min. For each heating rate six replicate measurements were performed. In addition the first replicate was scanned again at 10 °C/min immediately after the first scan. This second scan ensured complete cure during the first heating scan as evidenced by the absence of residual cure. DSC thermograms were then processed with the Mettler-Toledo STAR^e V7.2 software to extract the degree of cure, α, reaction rate, $d\alpha/dt$, and corresponding temperature, T_α, in the $0 \leq \alpha \leq 0.99$ range. Both α and $d\alpha/dt$ were determined at a specific cure time, t, by normalizing the partial heat of reaction, $\Delta H(t)$, and heat flow, dH/dt, respectively, by the total heat of reaction ΔH:

$$\alpha = \frac{\Delta H(t)}{\Delta H} \tag{1}$$

$$\frac{d\alpha}{dt} = \frac{dH/dt}{\Delta H} \tag{2}$$

MATLAB programs using the linear least square method were then developed to extract cure kinetic parameters according to the Friedman, Vyazovkin and KAS algorithms. The experimental data obtained at 2, 5 and 10 °C/min was then processed with these three programs. Kinetic parameters measured with the KAS algorithm were used to develop and compare dynamic cure predictions with experimental data at 20 and 25 °C/min. To further validate the three MFK methods for isothermal cure, isothermal DSC runs were conducted at 120 °C for different periods of time. The cure temperature and the cure times were selected based on experimental facility and so as to span the complete cure process. Specifically, the DSC cell was preheated to 120 °C and approximately 13.5 mg of PF resin was inserted and cured for different periods of time. The sample was then quickly removed from the DSC and quenched in liquid nitrogen. The residual heat of reaction of the partially cured samples, ΔH_R, was obtained from a subsequent ramp scan at 10 °C/min from 25 to 250 °C so that:

$$\alpha(t) = \frac{\Delta H - \Delta H_R}{\Delta H} \tag{3}$$

The total heat of reaction was taken as the average reaction heat previously measured in dynamic tests of fresh resins, 365 (±5) kJ/kg for PF-high and 420 (±9) kJ/kg for PF-low. The time dependence of the degree of cure at 120 °C was compared with predictions from the three methods.

2.3. MFK algorithms

The phenomenological kinetics of cure can be generally described as:

$$\frac{d\alpha}{dt} = A \exp\left(\frac{-E}{RT}\right) f(\alpha) \tag{4}$$

where $f(\alpha)$ is the reaction model, T (K) the absolute temperature, A (s^{-1}) the pre-exponential factor, E (kJ/mol) the activation energy and R the universal gas constant. The Friedman [16] Vyazovkin [14–15] and KAS algorithms [8–9] can then be used to determine the activation energy dependence on degree of cure E_α.

For various heating rates, β_i, the Friedman method directly evaluates Eq. (4) at a specific degree of cure α:

$$\ln\left(\frac{d\alpha}{dt}\right)_{\alpha i} = \ln(A_\alpha f(a)) - \frac{E_\alpha}{RT_{\alpha i}} \tag{5}$$

A new parameter $C_f(\alpha) = \ln(A_\alpha f(\alpha))$ can introduced so that $C_f(\alpha)$ and E_α are sufficient to fully describe the kinetic behavior:

$$\ln\left(\frac{d\alpha}{dt}\right)_{\alpha i} = C_f(\alpha) - \frac{E_\alpha}{RT_{\alpha i}} \tag{6}$$

For a specific α value and several heating rates β_i, pairs of $(d\alpha/dt)_{\alpha i}$ and $T_{\alpha i}$ are determined experimentally from the DSC thermograms. The parameters E_α and $C_f(\alpha)$ at this specific value of α are then estimated from plots of $\ln(d\alpha/dt)_{\alpha i}$ versus $1/T_{\alpha i}$ (Eq. (6)) across at least three different heating rates. The procedure is repeated for many values of α yielding continuous functions of α for E_α and $C_f(\alpha)$. The interest of the Friedman method is that Eq. (6) does not introduce any approximations and the method is not restricted to the constant heating rate mode. However, as in the case of any kinetic methods involving the differential term $d\alpha/dt$, the Friedman method is subject to significant numerical instability and noise interference [7].

As a result, Vyazovkin proposed an alternative algorithm, which is summarized in the following equations. A detailed derivation of the algorithm is provided elsewhere [14–15]. In Vyazovkin method n scans are performed at different heating programs $T_i(t)$. The activation energy at a specific degree of cure is obtained by minimizing the function $\varphi(E_\alpha)$:

$$\varphi(E_\alpha)=\sum_{i=1}^{n}\sum_{\substack{j=1\\(j\neq i)}}^{n}\frac{I[E_\alpha,T_i(t_\alpha)]}{I[E_\alpha,T_j(t_\alpha)]} \tag{7}$$

In Eq. (7) the temperature integral, I, is defined as:

$$I[E_\alpha,T(t_\alpha)]=\int_{t_{\alpha-\Delta\alpha}}^{t_\alpha}\exp\left(\frac{-E_\alpha}{RT(t)}\right)\mathrm{d}t \tag{8}$$

Eq. (8) can be solved numerically by integrating the experimental data within small time intervals $\Delta\alpha$. The I values are then substituted into $\varphi(E_\alpha)$, and this function is minimized by Brent's method [19] leading to E_α. Again the procedure is repeated for distinct values of α. A new parameter $C_v(\alpha)$ can also be created that complements E_α in fully describing the cure kinetics:

$$C_v(\alpha)=\int_0^\alpha\frac{\mathrm{d}\alpha}{Af(\alpha)}=\frac{1}{\beta}\int_{T_0}^{T}\exp\left(\frac{-E_\alpha}{RT}\right)\mathrm{d}T \tag{9}$$

Finally in the KAS method, E_α is evaluated by using Doyle's integral approximations in Eq. (10) [20]. In this case, Eq. (11) is derived for various heating rates. Again it can be rewritten into Eq. (12) by introducing a new parameter $C_k(\alpha)=\ln(RA_\alpha/E_\alpha g(\alpha))$:

$$g(\alpha)=\int_0^\alpha\frac{\mathrm{d}\alpha}{f(\alpha)}=\frac{A}{\beta}\int_{T_0}^{T}\exp\left(-\frac{E}{RT}\right)\mathrm{d}T\approx\frac{ART^2}{\beta E}\exp\left(-\frac{E}{RT}\right) \tag{10}$$

$$\ln\left(\frac{\beta_i}{T_{\alpha i}^2}\right)=\ln\left(\frac{RA_\alpha}{E_\alpha g(\alpha)}\right)-\frac{E_\alpha}{RT_{\alpha i}} \tag{11}$$

$$\ln\left(\frac{\beta_i}{T_{\alpha i}^2}\right)=C_k(\alpha)-\frac{E_\alpha}{RT_{\alpha i}} \tag{12}$$

The experimental determination of E_α and $C_k(\alpha)$ is similar to that of the Friedman method. For each degree of cure α, a corresponding $T_{\alpha i}$ and heating rate are used to plot $\ln(\beta_i/T_{\alpha i}^2)$ against $1/T_{\alpha i}$. The parameters E_α and $C_k(\alpha)$ are then determined from the regression slope and intercept, respectively.

The Friedman and Vyazovkin methods respectively solve the differential (Eq. (4)) and the integral kinetic forms (Eq. (8)) without approximations. On the other hand, the KAS method utilizes a close-form approximation (Eq. (10)). As a result, the KAS method provides only an estimate of the activation energy compared to the Vyazovkin and Friedman methods [21]. In addition, while the Friedman and Vyazovkin methods are applicable to different temperature programs, the KAS method only works for constant heating programs.

3. Results

3.1. Kinetic parameters from MFK methods

As expected, the commercial PF resoles exhibit two major exotherms that shift to higher temperatures with increasing heating rate (Fig. 1). In addition, PF-high displays a third intermediate exotherm of small intensity (Fig. 1). Hence, PF-low has two discernable cure reactions while three reactions are evident during PF-high cure. Note also that a high degree of cure (54%) is required for PF-low to reach its highest reaction rate while the maximum reaction rate is achieved very early (22% degree of cure) for PF-high. To interpret the differences in stages in the cure of both resins, the E_α dependence on degree of cure can be examined [22].

In Fig. 2, the dependence of E_α on degree of cure is computed from the Friedman, Vyazovkin and KAS algorithms. The

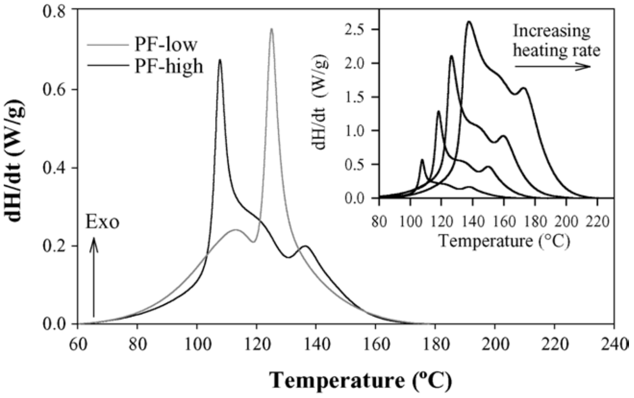

Fig. 1. DSC thermograms at 2 °C/min for the PF-low and PF-high resins. Insert highlights the influence of heating rate (2, 5, 10, and 20 °C/min) on the cure of the PF-high resin.

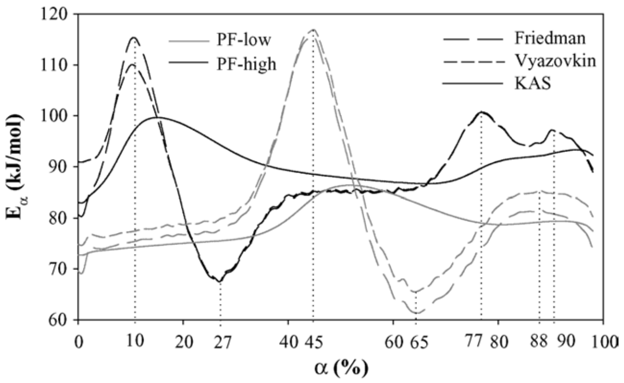

Fig. 2. Activation energies change with the degree of cure by the Friedman, Vyazovkin and KAS methods for the PF-low and PF-high.

overall range of activation energies between 60 and 120 kJ/mol is consistent with the values obtained from model fitting kinetics of PF resins [23–24]. Evident in Fig. 2 is the superposition of the Friedman and Vyazovkin E_α curves. The KAS method yields similar ascending and descending pattern, yet variations in E_α are smaller and the activation energy curve is shifted to higher conversion (Fig. 2). Such a consistency between the Friedman and Vyazovkin methods has been previously observed on simulated data of parallel reactions [15]. In contrast, the shift and low amplitude of E_α obtained with the KAS method likely stems from the approximation used in this algorithm. Recall that the Friedman and Vyazovkin methods use the point values of the overall reaction rate [21] or small time intervals [15] while the KAS method uses Doyle's approximation (Eq. (10)) that describes the history of the system [21]. Yet Vyazovkin reported that the KAS method provides satisfactory E estimates as long as E/RT is greater than 13 [25]. In the case of the commercial PF resoles used in this study, despite an $E/RT > 13$, the KAS method generates an activation energy curve that is shifted to higher conversion and reduced in amplitude. This discrepancy in the case of commercial PF resoles likely stems from violation of the Doyle's assumption of a constant activation energy across the kinetic process [11]. It results that the Vyazovkin and Friedman methods provide more consistent and accurate E_α functions. With these two methods, E_α is also more sensitive to changes in PF cure mechanisms. Therefore, to gain insight on the cure mechanism of PF resins, the Vyazovkin and Friedman methods are preferred over the KAS method.

Regardless of the method used the wavy shape of E_α points to the complexity and molecular weight dependency of PF cure kinetics. Indeed it is established that complex reactions involving multiple parallel reactions or changes in the limiting stage cause variations in E_α [26–28]. Specifically, an increasing E_α function reveals competition between parallel reactions [10,26]. Alternatively a concave decreasing E_α curve suggests a reversible stage reaction and a convex decreasing E_α function shows a change in limiting stage [26]. Therefore the shape of E_α can give some insight on the change in reaction steps [6].

For PF-low, Friedman and Vyazovkin methods generate two E_α peaks at 45 and 88% degrees of cure (Fig. 2) in accordance with two detected exotherms (Fig. 1). E_α shape for PF-low suggests four cure stages. The increasing and then concave decreasing E_α curve suggests the presence of competitive reactions up to 45% conversion followed by a reversible stage intermediate up to 65% [6,26]. At a degree of cure of 65% parallel reactions reconvene as indicated by the E_α increase until the cure changes from a chemical to a diffusion-controlled process [29] above 88% conversion where E_α decreases in a convex fashion [6,26]. This four-stage cure is more complex than the three-stage cure of PUF resins previously described based on the KAS algorithm [11]. Recall however that the KAS method is less sensitive to changes in E_α than the Vyazovkin and Friedman methods used in this study. In fact, the E_α curves obtained from the KAS method for PF-low and PF-high would also suggest a three-stage cure. In addition in contrast to a single cure exotherm previously detected on PUF resins [11], two exotherm peaks are detected on these commercial PF resoles.

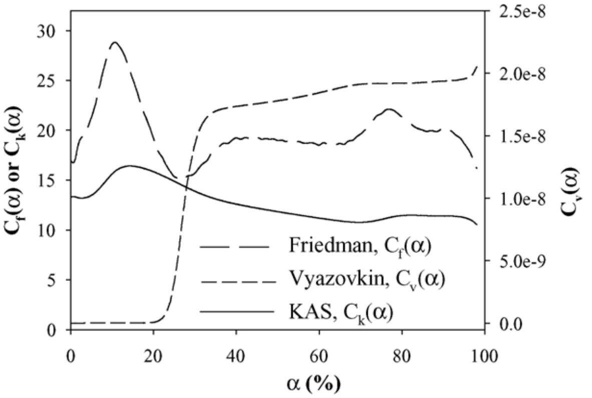

Fig. 3. Combined parameters of the Friedman, Vyazovkin and KAS methods for PF-high.

Although the specific reactions underlying the four stages cannot be identified solely based on this study, this cure behavior is in line with the individual cure reactions of urea-modified PF resins. PF cure involves a set of parallel reactions with HMPs formation, condensation and the various crosslinking chemistries [30]. With the addition of urea, condensation of phenol and urea with formaldehyde as well as co-condensation between phenol and urea derivatives are also taking place [31]. The changing contribution of each reaction to the overall activation energy explains the constant change in activation energy as cure progresses [11]. Since water is remains in the crucible during cure, the cure process is further complicated [12]. At low conversion water contributes to reversible reactions [12]. At high conversion, water plasticizes the PF network thus delaying diffusion control and allowing for more complete cure [12].

For PF-high an even more complex cure mechanism is observed with the presence of two highest E_α peaks at 10 and 77% conversion but also two small E_α peaks at 40 and 90% degree of cure. The greater complexity likely stems from the detection of three exotherms on the DSC thermogram for PF-high (Fig. 1). In all case PF-high likely exhibits a similar four steps pattern as PF-low does. That is competitive condensation reactions occur up to 10%; they are followed by a reversible intermediate stage up to 27% degree of cure. Competing crosslinking reactions then resume until diffusion rate control occurs at 77% degree of cure as previously observed on phenolic systems [10,11]. The E_α peaks shoulders at 40 and 90% may arise from a mathematical artifact.

Finally, the second MFK parameter needed to model reaction kinetics is the combined complex parameter $C(\alpha)$. The degree of cure dependence of this parameter with all three methods also reflects the changing cure mechanism as shown for PF-high (Fig. 3). Because this parameter is a modeling tool deprived of distinct physical meaning no inferences are made from its pattern. Next $C(\alpha)$ and E_α obtained from the three methods are utilized for assessing MKF predictions during dynamic and isothermal cure of PF resins.

3.2. Prediction of dynamic cure of PF resins

Eq. (12) used for the KAS method directly relates temperature and degree of cure [10]. Therefore, only the KAS method was

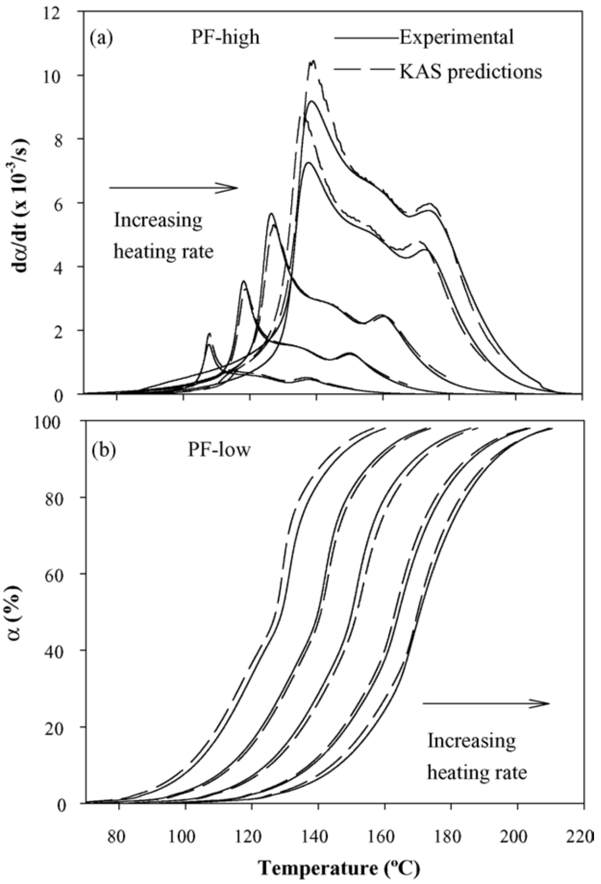

Fig. 4. Comparisons of experimental data and KAS predictions for dynamic conditions at 2, 5, 10, 20 and 25 °C/min for (a) the reaction rate of PF-high and (b) the degree of cure of PF-low.

used to predict the dynamic cure of PF resins. At a selected heating rate $C_k(\alpha)$ and E_α were substituted into Eq. (12) to predict the temperature associated with discrete values of α. An algorithm based on the Powell dogleg method [32] was developed with MATLAB to solve Eq. (12). Relationships between temperature and degree of cure were thus obtained and were easily converted to reaction rate-temperature relationships at specific heating rates. Fig. 4 compares experimental reaction rate and degree of cure with the KAS predictions for PF-high and PF-low respectively. Recall that the model was built from data at 2, 5, and 10 °C/min only whereas predictions are also made at 20 and 25 °C/min for model validation. Mean squared errors of prediction (MSEPs) [33] were calculated for both dynamic and isothermal MFK predictions (Table 1). The MSEP is the average squared difference between independent experimental observations and model predictions for the corresponding values of the independent variables [33]. The MSEP values of the KAS predictions for temperature and reaction rate are small, both one order of magnitude lower than those obtained with the best model-fitting kinetics in a parallel study [34]. The KAS method therefore provides excellent dynamic predictions compared to model-fitting kinetics. This is further evidenced in Fig. 4, where the KAS algorithm succeeds in capturing the complexity of PF-high thermogram.

Table 1
Mean squared errors of prediction for both dynamic and isothermal conditions at specific degree of cure and data points (in parentheses)

Predicted variable	Model	PF-low	PF-high
Dynamic (10 °C/min) temperature at α (°C)	KAS	2.97 (99)	0.27 (99)
Dynamic (10 °C/min) reaction rate at α (1/s)	KAS	9.82×10^{-8} (99)	6.27×10^{-8} (99)
Isothermal (120 °C) cure time at α (min)	Friedman	15.8 (11)	13.4 (13)
	Vyazovkin	16.7 (11)	19.1 (13)
	KAS	12.0 (11)	19.4 (13)

3.3. *Prediction of isothermal cure of PF resins*

Prediction of isothermal cure from dynamic scans is of scientific and practical interest. First, good prediction of isothermal cure from parameters obtained during dynamic cure clearly validates the models. Second, isothermal cure characterization is notoriously challenging from the experimental standpoint [35]. In this study, Friedman, Vyazovkin and KAS algorithms were used to predict the isothermal cure behavior of the two PF resins at 120 °C. The premise of isothermal prediction is that pairs of α and the corresponding $f(\alpha)$, $g(\alpha)$, E_α and A values are identical for dynamic and isothermal conditions [36]. Hence, MFK parameters can be used to develop a prediction model of the cure time needed to achieve a specific degree of cure, t_α, at a given temperature (T_{iso}).

With Friedman algorithm, Eq. (6) is rewritten to yield:

$$t_\alpha = \int_0^\alpha \exp\left(\frac{E_\alpha}{RT_{\text{iso}}}\right) \exp(-C_f(\alpha))\,\mathrm{d}\alpha \tag{13}$$

Vyazovkin method yields an integrated equation from Eqs. (4) and (9) at an arbitrary isothermal temperature T_{iso} as:

$$\int_0^t \exp\left(\frac{-E_\alpha}{RT_{\text{iso}}}\right)\,\mathrm{d}t = \int_0^\alpha \frac{\mathrm{d}\alpha}{Af(\alpha)} = C_v(\alpha) \tag{14}$$

At each small $\Delta\alpha$, the left integral is evaluated numerically with the trapezoid integration rule and the corresponding Δt is calculated. This calculation is reiterated from time 0 on. Thus at an arbitrary isothermal temperature a relationship between t_α and α is established.

Finally, the KAS parameters are used to reorganize Eqs. (4) and (12) into:

$$t_\alpha = \frac{R\exp\left(\frac{E_\alpha}{RT_{\text{iso}}}\right)}{E_\alpha \exp(C_k(\alpha))} \tag{15}$$

Isothermal cure predictions from all three MFK algorithms are compared with experimental data for PF-low and PF-high in Fig. 5. The small MSEP values (MSEP < 19.4) for both resins and all three models (Table 1) indicates the quality of the models compared to those determined in another study [34] from n-order kinetics (MSEP < 33). Analysis of variance (ANOVA) at an α level of 0.05 detected no differences in the isothermal prediction

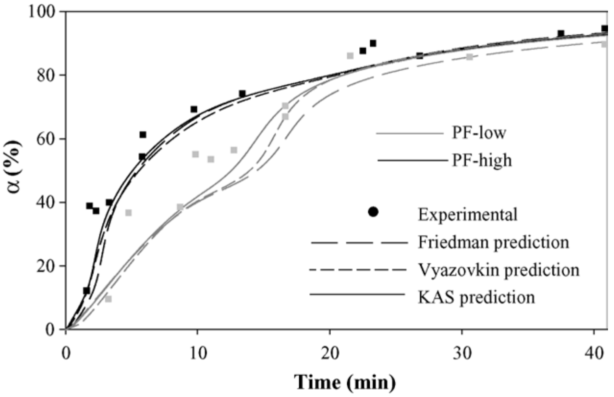

Fig. 5. Comparison of experimental data with the Friedman, Vyazovkin and KAS predictions of degree of cure of PF-low and PF-high during isothermal cure at 120 °C.

ability of the three MFK algorithms. Overall, the cure of PF-low and PF-high resins is equally well predicted with MFK methods. Yet, locally the isothermal data for PF-low does not capture the complexity of the cure prediction in the 10–20 min range (Fig. 5).

4. Conclusion

The cure development of two commercial PF resoles was analyzed by the Friedman, Vyazovkin and KAS model-free kinetics. The three algorithms were compared in their consistency and ability to perform dynamic and isothermal predictions. The Friedman and Vyazovkin methods generated consistent and accurate activation energy dependences on degree of cure. These two algorithms were also the most sensitive to changes in activation energy. Higher consistency and accuracy of the Friedman and Vyazovkin methods compared to the KAS algorithm were ascribed to the use of a close-form approximation of the kinetic equation in the latter algorithm. On the other hand, the KAS algorithm was more amenable to dynamic cure predictions. For isothermal cure predictions the three MFK algorithms provided equally good predictions. In all cases, predictions with MFK were significantly better than those measured in a parallel study with model-fitting methods. Hence, the Friedman and Vyazovkin methods are best suited for activation energy measurement. These two methods are the most appropriate for gaining insight on the cure mechanisms of commercial PF resoles. Alternatively, the KAS method is best suited for modeling and prediction purposes.

References

[1] A. Knop, L.A. Pilato, Phenolic Resins, Springer-Verlag, New York, 1985.
[2] R.B. Prime, in: E.A. Turi (Ed.), Thermal Characterization of Polymeric Materials, second ed., Academic Press, New York, 1997, pp. 1380–1744.
[3] P. Luukko, L. Alvila, T. Holopainen, J. Rainio, T.T. Pakkanen, J. Appl. Polym. Sci. 82 (2001) 258–262.
[4] T. Holopainen, L. Alvila, J. Rainio, T.T. Pakkanen, J. Appl. Polym. Sci. 66 (1997) 1183–1193.
[5] M.G. Kim, C. Watt, C.R. Davis, J. Wood Chem. Technol. 16 (1996) 21–34.
[6] S. Vyazovkin, C.A. Wight, Annu. Rev. Phys. Chem. 48 (1997) 125–149.
[7] N. Sbirrazzuoli, Y. Girault, L. Elégant, Thermochim. Acta 293 (1997) 25–37.
[8] H.E. Kissinger, Anal. Chem. 29 (1957) 1702–1706.
[9] T. Sunose, T. Akahira, Res. Report, Chiba Inst. Technol. 16 (1971) 22–23 (Sci. Technol.).
[10] G. He, B. Riedl, A. Aït-kadi, J. Appl. Polym. Sci. 87 (2003) 433–440.
[11] G. He, B. Riedl, J. Polym. Sci. B: Polym Phys. 41 (2003) 1929–1938.
[12] G. He, B. Riedl, A. Aït-Kadi, J. Appl. Polym. Sci. 89 (2003) 1371–1378.
[13] G. He, B. Riedl, Wood Sci. Technol. 38 (2004) 69–81.
[14] S. Vyazovkin, J. Comput. Chem. 18 (1997) 393–402.
[15] S. Vyazovkin, J. Comput. Chem. 22 (2001) 178–183.
[16] H.L. Friedman, J. Polym. Sci. C 6 (1964) 183–195.
[17] Y. Yazaki, P.J. Collins, M.J. Reilly, S.D. Terrill, T. Nikpour, Holzforschung 48 (1994) 41–48.
[18] D.W. Nelson, L.E. Sommers, in: A.L. Page (Ed.), Methods of Soil Analysis, Part 2. Chemical and Microbiological Properties, second ed., American Society of Agronomy, Madison, WI, 1982, pp. 539–579.
[19] R.P. Brent, Algorithms for Minimization Without Derivatives, Prentice-Hall, Englewood Cliff, NJ, 1973.
[20] C.D. Doyle, J. Appl. Polym. Sci. 5 (1961) 285–292.
[21] P. Budrugeac, E. Segal, Int. J. Chem. Kinet. 33 (2001) 564–573.
[22] N. Sbirrazzuoli, S. Vyazovkin, Thermochim. Acta 388 (2002) 289–298.
[23] R. Kay, A.R. Westwood, Eur. Polym. J. 11 (1975) 25–30.
[24] B.-D. Park, B. Riedl, Y.S. Kim, W.T. So, J. Appl. Polym. Sci. 83 (2002) 1415–1424.
[25] S. Vyazovkin, D. Dollimore, J. Chem. Inf. Comput. Sci. 36 (1996) 42–45.
[26] S.V. Vyazovkin, A.I. Lesnikovich, Thermochim. Acta 165 (1990) 273–280.
[27] J.H. Flynn, L.A. Wall, J. Res. Natl. Bur. Std. 70A (1966) 487–523.
[28] J. Opfermann, J. Therm. Anal. Cal. 60 (2000) 641–658.
[29] J.B. Butt, Reaction Kinetics and Reaction Design, second ed., Marcel Dekker Inc., New York, 1999.
[30] W.D. Detlefsen, in: M. Chaudhury, A.V. Pocius (Eds.), Surfaces, Chemistry and Applications, Elsevier, Amsterdan, 2002, pp. 869–945.
[31] G. He, N. Yan, Polymer 45 (2004) 6813–6822.
[32] M.J.D. Powell, in: P. Rabinowitz (Ed.), Numerical Methods for Nonlinear Algebraic Equations, Gordon and Breach Science Publishers, London, 1970, pp. 87–114.
[33] J.O. Rawlings, S.G. Pantula, D.A. Dickey, Applied Regression Analysis, second ed., Springer, New York, 1998.
[34] J. Wang, M.P. Laborie, M.P. Wolcott, J. Appl. Polym. Sci. 2005, Submitted for publication.
[35] G. Widmann, Thermochim. Acta 11 (1975) 331–333.
[36] C.D. Doyle, J. Appl. Polym. Sci. 6 (1962) 639–642.